Intraday trader lead-lag networks and order flow prediction

Damien Challet[1,2], Rémy Chicheportiche[3,4], Mehdi Lallouache[5], Serge Kassibrakis[6]

[1] Laboratoire MICS, CentraleSupélec, Université Paris Saclay, 92290 Châtenay-Malabry, France

[2] Encelade Capital SA, 1015 Lausanne, Switzerland

[3]Capital Fund Management, 75007 Paris, France

[4] previously at Swissquote Bank SA, 1196 Gland, Switzerland

[5] Mosaic Finance, 75008 Paris, France

[6]Swissquote Bank SA, 1196 Gland, Switzerland

February 9, 2017

arXiv:1609.04640v2 [q-fin.TR] 8 Feb 2017

Abstract

Using trader-resolved data, we bring to light lead-lag activity networks between groups of investors in the foreign exchange market at an hourly time scale. Because these relationships are systematic and persistent, they allow order flow prediction. We thus propose a generic method to exploit trader lead-lag and predict the sign of the total order imbalance over a given time horizon. It first consists in an unsupervised clustering of investors according to their buy/sell/inactivity synchronization. The collective actions of these groups and their lagged values are given as inputs to machine learning methods. When groups of traders and when their lead-lag relationships are sufficiently persistent, highly successful out-of-sample order flow sign predictions are obtained.

1 Introduction

Internal order crossing may occur if incoming orders can be matched against current inventory or added to it. It may happen at many levels. For example, two strategies of an investor may have opposite opinions about the same asset at about the same time, in which case internal crossing saves transaction fees and reduces uncertainty. If an order needs to be sent to an exchange, it may be matched on its way at crossing networks, dark pools, or even at an internal matching system within the exchange (e.g. IMS at NYSE Euronext) [Harris, 2002].

Managing one's inventory in this situation is of great practical importance. A standard approach would be to solve an optimization problem. We consider this situation as a prediction problem instead and show how being able to identify the source of orders makes the order flow predictable after suitable filtering.

Accordingly, we focus here on matching engines that are able to identify the source of the order (strategy, investor, broker, etc.). Prediction in our framework rests on the existence and persistence of trader lead-lag networks in which the activity of a trader (e.g. buy) systematically leads on that of an other trader (e.g. sell). We thus introduce an unsupervised method to infer such networks that may be applied at all levels of order crossing and in a non-financial context in which the similarity of choices of items by customers may be used to predict future actions. The method rests on the fact that some investors are active and inactive in a remarkably synchronous way and may therefore be classified into a finite number of groups [Tumminello et al., 2012]. Our first contribution is to extend the algorigthm of Tumminello et al. [2012] to detect systematic lead-lag between the actions of groups of traders. While synchronicity is likely due to the use of the same strategies or of the same source of information, or both, lead-lag networks are likely caused by the different reaction speed of the respective strategies (e.g. two moving averages with different parameters); an alternative explanation is that some traders react with different delays to common information [Boudoukh et al., 1994, Jegadeesh and Titman, 1995].

If these lead-lag networks are sufficiently persistent, order flow is predictable if one knows that the states of leading groups during a given time slice. Our second main contribution is thus to illustrate this point. Only the simplest prediction scenario is studied: we try to predict the sign of the future order flow from the global state (buy, sell, neutral) of each trader group. In other words, we reduce order flow prediction to a classification problem from discrete variables and use standard methods of machine learning. Although seemingly crude, this setup leads to significant out-of-sample performance for the prediction of the order flow itself.

1.1 Literature review

Our contribution is related to several areas of finance pertaining to order flow segmentation, predictability, and inventory control by an informed market maker.

The first broad related area is market making in the presence of predictable order flow. In the context of market microstructure, the role of meta-orders in the long memory of the sign of market orders is well documented [Lillo and Farmer, 2004, Bouchaud et al., 2009]. The order flow of individual traders is known to be anti-correlated with previous daily or weekly price returns [Grinblatt and Keloharju, 2000, Kaniel et al., 2008]. A related topic, although less directly relevant to our contribution, is the predictive power of order flow on other quantities than itself such as price returns [Kelley and Tetlock, 2013]. Whereas market maker were assumed to be fighting against informed traders in the early literature, the long memory of market order signs leads to a new paradigm of optimal market making [Avellaneda and Stoikov, 2008]. Internal order matching differs from market making at an exchange in that one may liquidate in part one's inventory at the exchange, although with non-negligible transaction costs [Gallien et al., 2016].

Trader grouping is often performed according to their role in financial markets (e.g. individual investor, institutional investor, etc). Average properties are then computed over whole sub-populations [Grinblatt and Keloharju, 2000, Jackson, 2004, Grinblatt and Keloharju, 2009, Barber et al., 2009]. Unsupervised clustering on the other hand rests on the similarity of actions of traders determined *ex post*. The simplest approach is based on the computation of the correlation matrix of trader inventory changes; Then Principal Component Analysis is used together with Random Matrix Theory to extract eigenvalues outside the random spectrum [Zovko and Farmer, 2007, Lillo et al., 2008, Zhou et al., 2012]. It turns out that at a timescale of a single day, only one or two eigenvalues stand out of the noisy bulk, the largest being associated with previous price returns. This allows one to classify traders as mean-reverting (the majority of them), trend-following, and non-classifiable. The drawback of this approach is that of linear correlations that do not capture the full correlation structure of traders. In addition it fixes the number of categories of traders.

An alternative approach is Statistically Validated Networks (SVNs) [Tumminello et al., 2011] which consists in computing a similarity score between two traders according to how synchronous and similar their activity and inactivity are. This allows one to determine a p-value of synchronousness and to establish a link between two traders in a statistically sound way. Once all the links between all pairs of traders are tested, one obtains the full synchronousness network of traders. Tumminello et al. [2012] find a surprising degree of synchronization between within groups of Finnish traders at a daily timescale.

Lead-lag relationships between traders are much less studied. For lack of available data, the literature has focused on lead-lag relationships between price returns [Kullmann et al., 2002, Tóth and Kertész, 2006, Huth and Abergel, 2014, Curme et al., 2015]. Lead-lag relationships between traders are discussed in the context of various time scales of contrarian behavior [Boudoukh et al., 1994, Jegadeesh and Titman, 1995]. We are not aware of any work on unsupervised inference of lead-lag between traders.

2 Data description and notations

We work with datasets on foreign exchange (FX) transactions from two independent sources: a large dealing bank (LB hereafter[1]), and a broker-dealer (Swissquote Bank SA, SQ hereafter[2]). The reader might

[1] LB's electronic market-marking desk provides liquidity (i.e. quotes and volumes) on the currency rates to large clients such as commercial companies, financial institutions, pension funds, hedge-funds.

[2] SQ acts as an on-line broker on thousands of financial instruments, with a large market share in the global Foreign eXchange activity in Switzerland. Its clients range from retail investors to asset managers and institutions.

Dataset	Timespan	Instruments	Traders	Trades
SQ 2012	31 Jan. 2012 → 10 Aug. 2012	68	$> 10^3$	$> 10^6$
SQ 2014-6	01 July 2014 → 15 March 2016	206	$> 10^4$	$> 10^7$
LB	01 Jan 2013 → 17 Sep. 2014	12	$> 10^4$	$> 10^6$

Table 1: Basic statistics of the datasets.

Dataset	Pair	Traders	Trades
SQ 2012	`EURUSD`	$> 10^3$	$> 5 \times 10^5$
SQ 2014-6	`EURUSD`	$> 10^4$	$> 10^6$
	`EURGBP`	$> 5 \times 10^3$	$> 5 \times 10^5$
	`USDJPY`	$> 10^4$	$> 10^5$
LB	`EURUSD`	7300	5×10^5

Table 2: Basic statistics of the datasets for the three studied pairs.

refer to Harris [2002] for details about the FX market organization. All datasets contain information about all the trades of their clients over a given period: anonymous client identification number, trade time with a millisecond precision, traded currency pair, signed volume, and price (currency rate). A summary of the datasets structure and contents is provided in Table 1.

This paper focuses on the most traded pairs only. Accordingly, Table 2 gives a breakdown of descriptive statistics of the studied pairs. For confidentiality reasons, we cannot give more precise figures for SQ.

2.1 Number of transactions per trader

The number of transactions n per trader per year for a given asset in equity markets has been reported to have heavy tails which may be approximated by a power-law $P(n) \sim n^{-\alpha}$ with tail exponent $\alpha \simeq 2$ [Tumminello et al., 2012]. This means that some traders are orders of magnitude more active than others, which implies that focusing on the most active traders may simplify much the prediction of future order flows. We checked that the power-law still holds on FX markets over about 2 decades of n; the exponent α was estimated for each currency and each year with the method introduced by Clauset et al. [2009] (see also Gillespie [2015]). For a given currency pair, we filtered out the years in which less than 1000 traders were active, which left 53 estimates. We found $\alpha_{avg} \simeq 1.99 \pm 0.07$ (95% confidence interval) in the largest dataset (SQ 2014-6).

2.2 Trade size

The different nature of the respective clients of LB and SQ influences the typical trade size. We present the results in multiple of 1000 of the base currency for SQ clients and in multiple of $100'000$ for LB clients. In Fig. 1, we plot the distribution of the transaction sizes for the `EURUSD`. Similar results are obtained for other pairs. We observe peaks at round size (10,20,50,...), with a stronger effect for SQ than for LB, which is consistent with the fact that its clients are mostly individual traders, therefore more prone to be affected by psychological biases than institutional traders (see a discussion about this phenomenon in the FX EBS market in Lallouache and Abergel [2014]).

3 Outline

The structure and rationale of this paper are as follows

1. Introduction of an unsupervised inference method of lead-lag activity networks. It consists in two steps

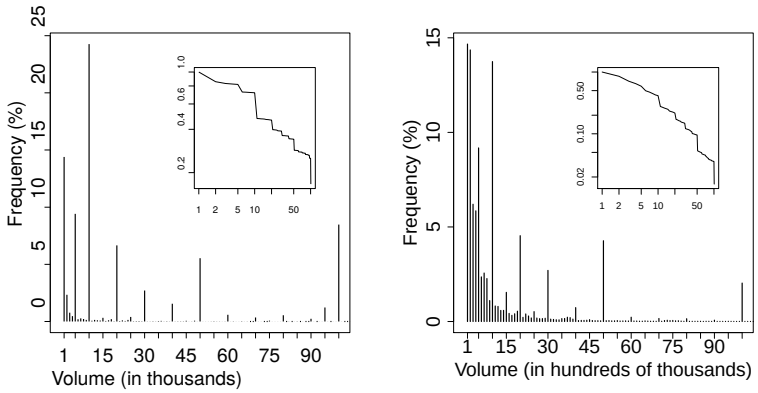

Figure 1: Distribution of `EURUSD` trade sizes. Left: SQ. Right: LB. Inset: cumulative tail distribution, in log-log scale.

(a) Unsupervised trader clustering: groups of traders are determined according to the synchronicity of their activity.

(b) Inference of group lead-lag networks. Two groups are linked if the activity of one group predicts that of the other one.

2. Order flow prediction: the activity states (buy/sell/neutral) of the groups thus determined in point 1.b and their lagged values are given as inputs to machine learning methods, which are then trained to predict the sign of order flow.

4 Inference of trader lead-lag networks

4.1 Trader activity unsupervised clustering

4.1.1 Method

Statistically Validated Networks (SVN) were introduced in [Tumminello et al., 2011] and applied to the clustering of Finnish investors in Tumminello et al. [2012]. The technique aims at characterizing the degree of synchronization between the actions of two traders, thus, by extension, at identifying groups of traders who act in a similar way. By definition, it is an unsupervised clustering method.

The first step is to cut time into slices of equal length δt; we chose arbitrarily $\delta t = 1$ hour. In practice, the duration of each slice must be adapted to each situation. In the case of the FX traders in our dataset, 1 hour is a reasonable choice with respect to typical trading patterns of active traders. We define time slice t as the interval $[t, t + \delta t[$. For each time slice t, we classify the state of all traders into buying (state +1), selling (state -1), neutral (state 2), and inactive (0). Denoting the total signed volume of trader i during time slice t by $V_i(t)$ and the sum of the absolute trading volume of the transactions of trader i during time slice t by $G_i(t)$, one defines the imbalance ratio $\rho_i(t) = V_i(t)/G_i(t)$. The imbalance ratio characterizes the trader as a net buyer ($\sigma_i(t) = 1$) if $\rho_i(t) > \rho_0$ (ρ_0 being a small threshold), as a net seller ($\sigma_i(t) = -1$) if $\rho_i(t) < -\rho_0$, as neutral ($\sigma_i(t) = 2$) if $|\rho_i(t)| < \rho_0$, or as inactive ($\sigma_i(t) = 0$) if $V_i(t) = G_i(t) = 0$. The choice of $\rho_0 \in [0.01, 0.1]$ is not crucial; in the following we set $\rho_0 = 0.01$. Because the following analysis focuses on the most active traders, the inactive state will be dropped.

Synchronicity of a pair of traders is measured by counting the co-occurrences in the time series of their states, and attributing a p-value that reflects the statistical significance of this synchronicity assuming pure randomness. To deal with the testing of all pairs of traders for each of the 9 types of co-occurrences of states $\{-1, 2, 1\} \times \{-1, 2, 1\}$, a multiple hypothesis testing correction is needed. We choose to use the False Discovery Rate [Benjamini and Hochberg, 1995] with a rate set to $p_0 = 0.05$. A network is built by validating links between pairs of traders if the p-value of their synchronization is smaller than the FDR-corrected threshold (see Tumminello et al. [2012] for more details).

The resulting network consists most of the time in a large connected component (i.e. a large group of connected traders) and other very small disconnected components. The large connected component is further decomposed into communities (or modules). Many methods have been designed to detect communities in complex networks (see e.g. Lancichinetti and Fortunato [2009] for a review). As in Tumminello et al. [2012], we use the InfoMap method [Rosvall and Bergstrom, 2008], which segments a connected network according to a maximum entropy argument. While this method is not suited for multi-links networks, it can deal with weighted networks. Therefore an easy workaround consists in converting multi-links into weighted links by assigning a weight equal to the number of validated links between two traders. When applying community detection, we exclude links between opposite action (buy-sell), as we are primarily interested in finding groups with that trade in the same direction at the same time so as to be able to aggregate the volume of a given group and compute a meaningful measure of its state.

4.1.2 Trader network descriptive statistics

In the following, for each in-sample time window, we keep the 500 most active traders and filter out those with less than 100 trades. We exclude weekends as trading activity then is markedly different (and much smaller) than that of business days. In addition, some traders do not use algorithmic trading, which restricts their activity periods, or prefer to trade during the most active hours. This is why we only keep trades from 9am to 4pm (London time).

Hourly time slices also allow the building of SVNs over a few months instead of a full year, which opens the way to a large-scale investigation both of the time evolution of SVNs and of order flow prediction (see Sec. 6). Fig. 2 shows representative examples of SVNs computed with hourly time slices over a given time period. The number of clusters is of particular interest: while the number of groups of SQ traders stays roughly constant (and large), a peculiar phenomenon occurs in the four months preceding Jan. 2014 in the LB dataset: Fig. 3 reports that the number of detected groups reaches 1 then, with a similar decrease of the number of links between traders. This implies that our method detected much less statistically validated synchronization during this period. We were not able to find a simple explanation for this phenomenon, but it is clear that the presence of a single group prevents significant lead-lag. We thus expect predictability to be minimal around January 2014 for LB data (which is confirmed in section 6.2).

4.1.3 Stability of clustering as a function of time

Sliding windows allow us to detect time-varying clustering, which reflects changes of strategy use by the traders as time goes on. They also raise the question of the stability of clustering, a necessary condition for the persistence of lead-lag networks, thus for the possibility of predicting order flows.

Assessing clustering stability is made easier by having consistent group labeling. The first step is to make sure that the clustering tools guarantees the constant labeling of groups when the grouping of traders is exactly the same one between two time slices. In practice, a non-negligible proportion of traders do not belong to the same group in the clustering performed at two consecutive times. Thus, the first problem to solve is how to attribute coherent names to clusters as time goes on. The simplest solution is to use a similarity measure between of the grouping at time slices t and $t-1$ and to propagate the name of cluster g_{t-1} to the most similar cluster at time t. The similarity measure is based on the overlap of the elements of two clusters and defined as

$$OA(g_{t-1}, g'_t) = |g_{t-1} \cap g'_t| \,, \tag{1}$$

where g and g' are trader groups/clusters and where $|x|$ stands for the number of elements of x. We shall use the normalized overlap measure

$$OP(g_{t-1}, g'_t) = \frac{OA(g_{t-1}, g'_t)}{|g_{t-1} \cup g'_t|} \tag{2}$$

to account for the size of both clusters.

Consistent naming allows us to produce meaningful visualizations. Fig. 4 shows how the traders switch between clusters as a function of time, using a so-called "river chart": at a given time, the traders

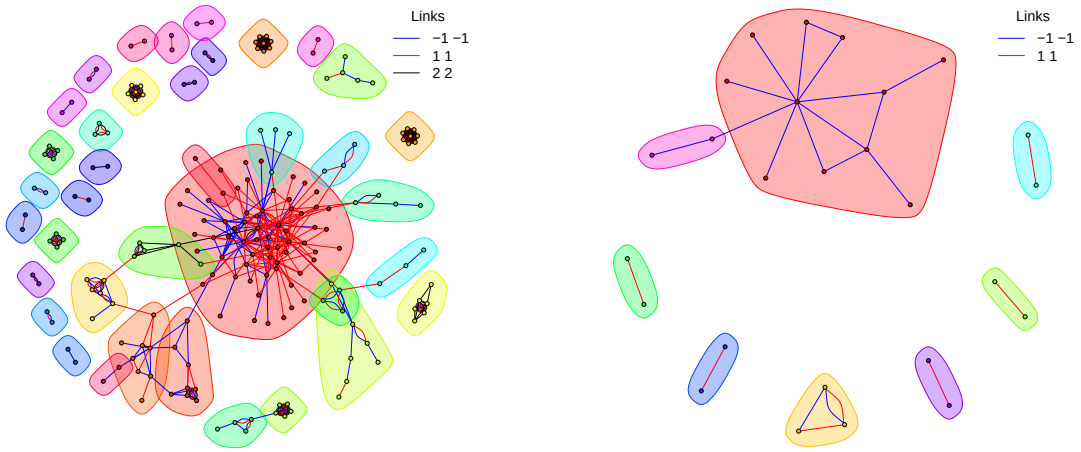

Figure 2: Projection of typical networks of traders, determined at the hourly time scale (EURUSD). Every link between two traders is statistically validated and labelled by the equal-time behavior of the pair: (1,1) if both are net buyers, (-1,-1) if both are net sellers, (2,2) if both are neutral. The InfoMap community detection method additionally provides coloured clusters. Left: SQ 2012. Right: LB.. These are bi-dimensional projections of complex networks in which horizontal and vertical directions have no special meaning.

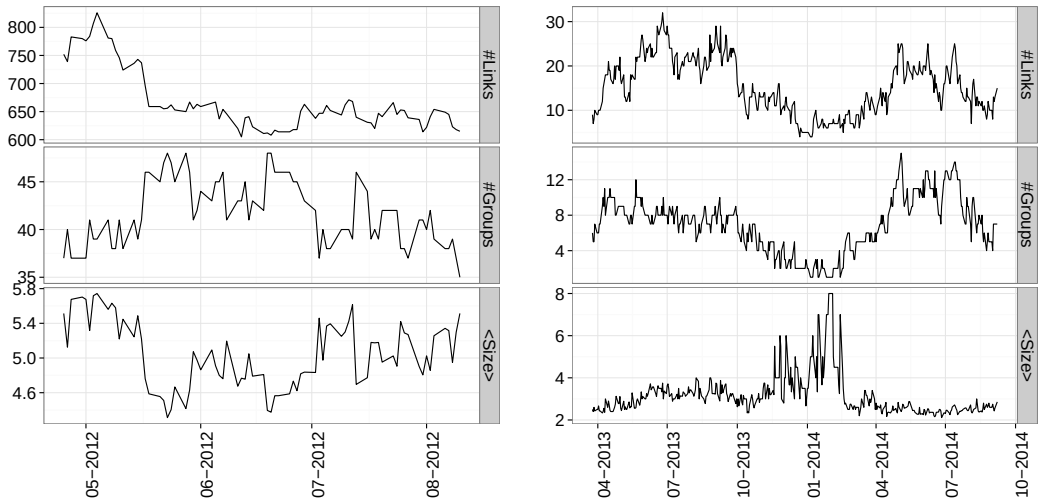

Figure 3: Network of traders: basic statistics over time (EURUSD). Left: SQ 2012. Right: LB.

mean(std dev)	LB EURUSD	SQ EURUSD	SQ EURGBP	SQ USDJPY
mean	0.87	0.83	0.91	0.84
standard deviation	0.14	0.09	0.09	0.10
fraction of perfect stability	0.34	0	0.01	0

Table 3: Summary statistics of the Adjusted Rand Index for some currency pairs of both data sources. SQ means SQ2014-6.

belonging to the same group are stacked together and form a continuous vertical dash, each group being clearly separated from each other. One then adds the trajectory of each trader from its group at times t and its group at time $t+1$. Having a consistent group labeling method ensures that if there is strictly no change of group between two time steps, only horizontal stripes appear. Thus, river charts allow us to visualize at the same time group sizes and the evolution of group compositions, i.e. distributional and dynamical properties. There clearly is a large cluster whose size is relatively stable as a function of time. The smallest clusters are much less stable: they merge and split again as time goes on. It is noteworthy that clustering was performed every week in this figure: the cluster structure is relatively stable even at this sampling frequency.

4.1.4 Cluster membership stability

Because the cluster labels are determined in a meaningful way, one can use the Adjusted Rand Index (ARI thereafter), a standard global measure of clustering stability, used here between two consecutive clustering times [Rand, 1971, Fraley et al., 2012]. An ARI of 1 denotes perfect clustering stability, while the expected value of ARI for random clustering is 0. The stability of LB traders is perfect (ARI=1) in about a third of the days, which underscores a remarkable level of regularity of LB clients, also hinted at by the large average ARI. Retail clients of SQ are more fickle (possibly because some of them do not use algorithmic trading), but their average ARI is also remarkably high (see Table 3). In short, the ARI suggests a strong and encouraging level of clustering stability in all data sets.

5 Hourly trader lead-lag relationships

This section is devoted to documenting the existence of significant and persistent lead-lag relationships between traders, which mechanistically implies the possibility of aggregate investment flow prediction.

Determining validated lead-lag relationships between two time-series is very much the same as detecting synchronicity between the first time series and the suitably lagged second time series. Accordingly, we may use once again the SVN machinery with a new tweak. The key ingredient is to focus on lead-lag relationships between the previously determined groups of traders. Indeed, since traders belonging to the same group trade significantly in the same direction synchronously, it makes sense to aggregate the volume of their transactions.

Once the groups of traders are determined via the SVN method, the procedure works as follows:

1. volume imbalances are aggregated at the group level: $V_g(t) = \sum_{i \in g} V_i(t)$ and the state of group g, denoted by $\sigma_g(t)$, is determined in the same way as in the SVN method;

2. for each pair of group (g, g') ($g = g'$ is allowed), the p-value of the coincidence between $\sigma_g(t)$ and $\sigma_{g'}(t+1)$ is computed as in the SVN method;

3. the number of pairs of groups is N^2_{groups} because we allow self-linking. Since the number pairs of states is 3x3, the significance level needs to account for $N_{tests} = 9 \times N^2_{groups}$ tests, thus FDR is used once more. Notice in particular that $g \to g$ links are not trivial and correspond to auto-correlated time series of aggregated volume imbalance: these links appear as loops in the directed network representation.

5.1 Results

The same parameters as in Fig. 2 are used for link detection between groups. We display two representative networks in Fig. 5. The most common type of link is to oneself. More complex lead-lag relationships also exist: take group 22 in SQ data set; it typically buys `EURUSD` within one hour after having sold `EURUSD`; group 31 does the opposite. One notes that, quite expectedly, group 31 sells during the hour after group 22 has sold. This means that both groups act in an opposite way provided that group 22 has sold `EURUSD` in the previous time slice. What is remarkable is this happens in a remarkably systematic way.

More links are present for SQ compared to LB, especially self-links. Interestingly, more links that validate opposite directions are present in the lead-lag case compared to the contemporaneous one. The evolution of the number of links over time is shown in Fig. 6: sudden drops of the number of lead-lag links are noticeable for all data sets of SQ. Quite logically, there is no lead-lag relationships around January 2014 for the LB dataset, which is to be related to the detection of only one group (see Fig. 3).

The presence of links, valid under severe statistical inspection, clearly demonstrate the existence of predictability in the investors trading directions. However, predicting trading flows not only requires equal-time clustering stability, but also lead-lag stability. Measuring the latter at the level of traders is much more informative than only using lead-lag between groups. Indeed, imagine that at time t, group 1 includes Alice and Bob, and leads on group 2 which contains Carol and Dave. It may happen that at time $t+1$ group 1 splits into groups 1a and 1b, that the composition of group 2 is conserved, and that groups 1a and 1b still lead on group 2. The point here is that the lead-lag between group 1 and 2 defines *a fortiori* lead-lag relationships between all the traders of group 1 and those of group 2 at time t. The subsequent splitting of group 1 into 1a and 1b does not change the lead-lag relationships between traders. Thus, a suitable lead-lag stability measure is the fraction of lead-lag links between traders that is conserved between two successive clustering times, restricted to the traders that exist at both times. Mathematically, let $\Lambda_{ij}(t \to t+1)$ denote the adjacency matrix element of the lead-lag network at the trader level between time t and time $t+1$, i.e., $\Lambda_{ij}(t \to t+1) = 1$ if trader i leads on trader j and 0 otherwise, then the stability measure is defined as

$$\beta(t \to t+1) = \frac{\sum_{ij} \Lambda_{ij}(t \to t+1)\Lambda_{ij}(t+1 \to t+2)}{\sum_{i'j'} \Lambda_{i'j'}(t \to t+1)}$$

Figure 7 reports the time evolution of β. It does fluctuate much, but never quite reaches 0 for long periods, except for LB in January 2014, which, once again, leaves hope of successful predictions. Whether a high value of β is related to a larger predictive power is investigated in Sec. 6.3.

6 Order flow prediction

We have so far shown the existence of a lead-lag structure whose persistence implies that order flow is predictable. This means that order flow prediction is simplified by exploiting this structure.[3] As a consequence, the prediction must exploits at time t the states of the groups at time t and their values lagged once. For the sake of simplicity, we have restricted the states to their discrete values {-1,2,+1}. This strongly suggests to predict the sign of the total order flow, instead of its exact value.

More precisely, we aim to predict $s(t+1) = \text{sign}(\sum_i V_i(t+1))$, where i sweeps over all the traders, of the aggregated trading flow imbalance during the next time slice, i.e. classify $\hat{s}(t+1)$ into $\{-1, 0, +1\}$, from the knowledge of group states up to time t.

6.1 Methods

6.1.1 Predictors and training phase

The aim is to predict $s(t+1)$ from a set P of predictors consisting in the states of the groups, denoted by $\sigma_{g,t}$ (determined in-sample by SVNs), their lagged values $\sigma_{g,t-1}$ and the hour of the day. Including

[3] We tried to fit ARIMA models at an hourly time scale, without any success. The AIC criterion always suggests to use a ARIMA(0,0,0) model: in short, at this time scale, the only relevant factors are the hours of the day.

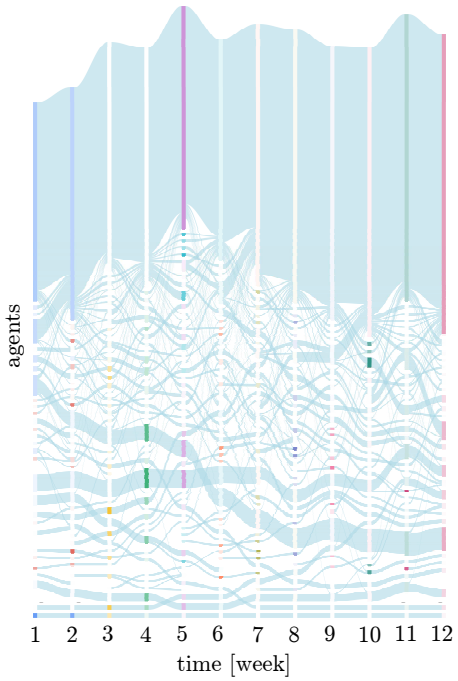

Figure 4: Agent clustering time evolution. Each elementary line width represents the trajectory of an agent from one group to an other group. Hourly time slices, 12 weeks in-sample, weekly clustering; SQ 2012, `EURUSD`.

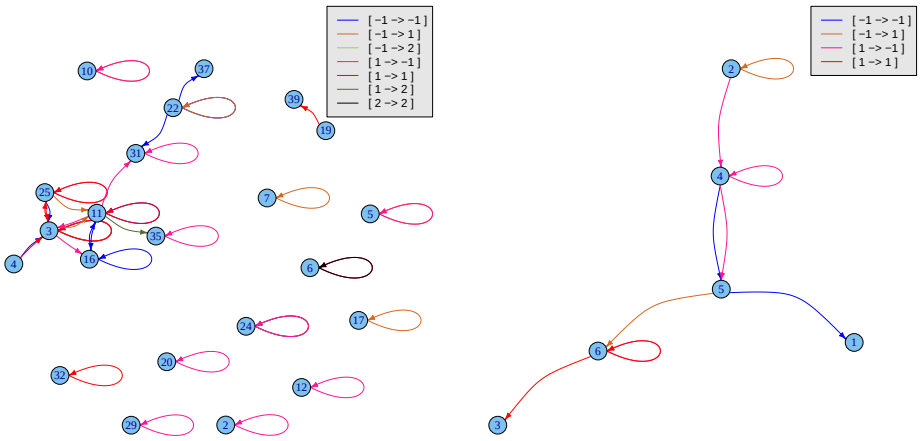

Figure 5: Examples of lead-lag networks between groups at an hourly scale, for a given given date and a calibration window of 50 days (`EURUSD`, left: SQ, right: LB). 2 labels the neutral state.

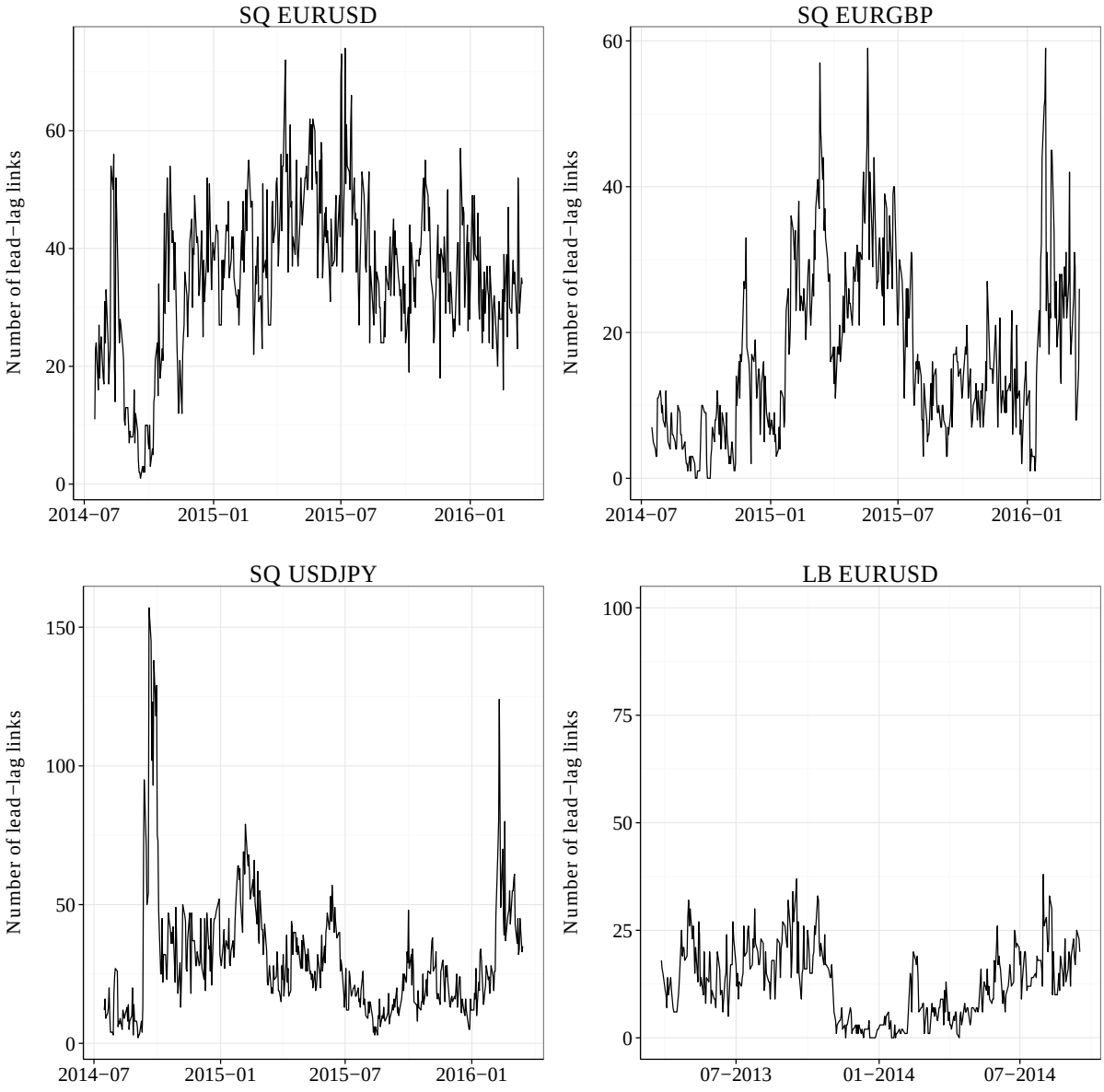

Figure 6: Lead-lag network of traders: number of links as a function of time. Sliding windows of 45 days of calibration.

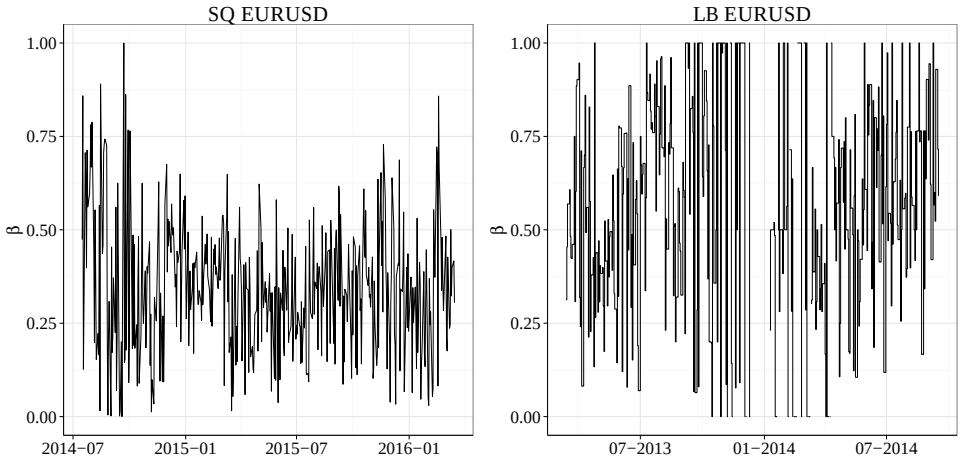

Figure 7: Trader-trader lead-lag overlap ratio β as a function of time. Same parameters as in Figure 6.

lagged group states is consistent with the existence of group lead-lag of order one.

The training phase is summarized by $P_{t_0,t_1} \sim v_{t_1+1}$, where P_{t_0,t_1} is a matrix of predictors and v_{t+1} the vector of the quantity to be predicted; more precisely,

$$P_{t_0,t_1} = \begin{pmatrix} \sigma_{1,t_0} & \sigma_{2,t_0} & \sigma_{1,t_0-1} & \sigma_{2,t_0-1} & h(t_0) \\ \vdots & \vdots & \vdots & \vdots & \vdots \\ \sigma_{1,t_1} & \sigma_{2,t_1} & \sigma_{1,t_1-1} & \sigma_{2,t_1-1} & h(t_1) \end{pmatrix} \sim \begin{pmatrix} \hat{s}_s(t_0+1) \\ \vdots \\ \hat{s}_s(t_1+1) \end{pmatrix} = v_{t+1}, \tag{3}$$

where the symbol $\sim$ implies that there is some kind of (possibly highly non-linear) relationship between a line of P_{t_0,t_1} and the corresponding next global trading flow imbalance, as suggested by the validated lead-lag networks plotted in Fig. 5. Because P_{t_0,t_1} also contains the time of the day, subtle hourly differences of these validated lead-lag networks may be detected as well. Note that P_{t_0,t_1} can also include group states lagged more than once. Many variations of Eq. (3) are relevant. First, instead of the group states, one can input the actual volume (or log-volume), v may also be the VWAP or future price returns, etc. At all rates, we focus on the simplest possible setting here.

This setup suggests to infer the $\sim$ relationship with logistic regression, which does not lead to satisfactory results (see appendix A where they are reported). Off-the shelf machine learning methods outperform logistic regression thanks to their more non-linear nature; we thus will focus on such methods. Instead of trying and comparing many machine learning methods and tuning their parameters until seemingly finding predictability, we chose a single method known for its robustness and performance: plain random forests (RF) [Breiman, 2001, Ishwaran and Kogalur, 2016], which have many useful features in this context: first, they avoid in-sample over-fitting, they are robust, non-linear and possess an overall very good predictive power without tweaking any parameter (at least on many "standard" data-sets [Fernández-Delgado et al., 2014]). A bonus is the availability of the relative importance of each predictor. As a consequence, we will be able to check that group states, i.e., lead-lag, is on average more important than the time of the day. For the sake of computation speed, calibration was performed every day, not every hour. Thus, predictions for a given day rest on a calibration that uses data up to the previous day.

We choose 10 calibrations window lengths, denoted by T_{in}, ranging from 45 to 90 week days (9 to 18 weeks) with common difference of 5 days (1 week). Although RFs output classification probabilities, i.e., the probability that the sign of the next order flow will be $+1$, say, we choose the most probable sign as the prediction of a given RF. In addition to computing the respective performance of each calibration length, we also performed a majority vote of the predictions originating from each timescale. If $+1$ and -1 obtain the same number of votes, the prediction is set to zero .

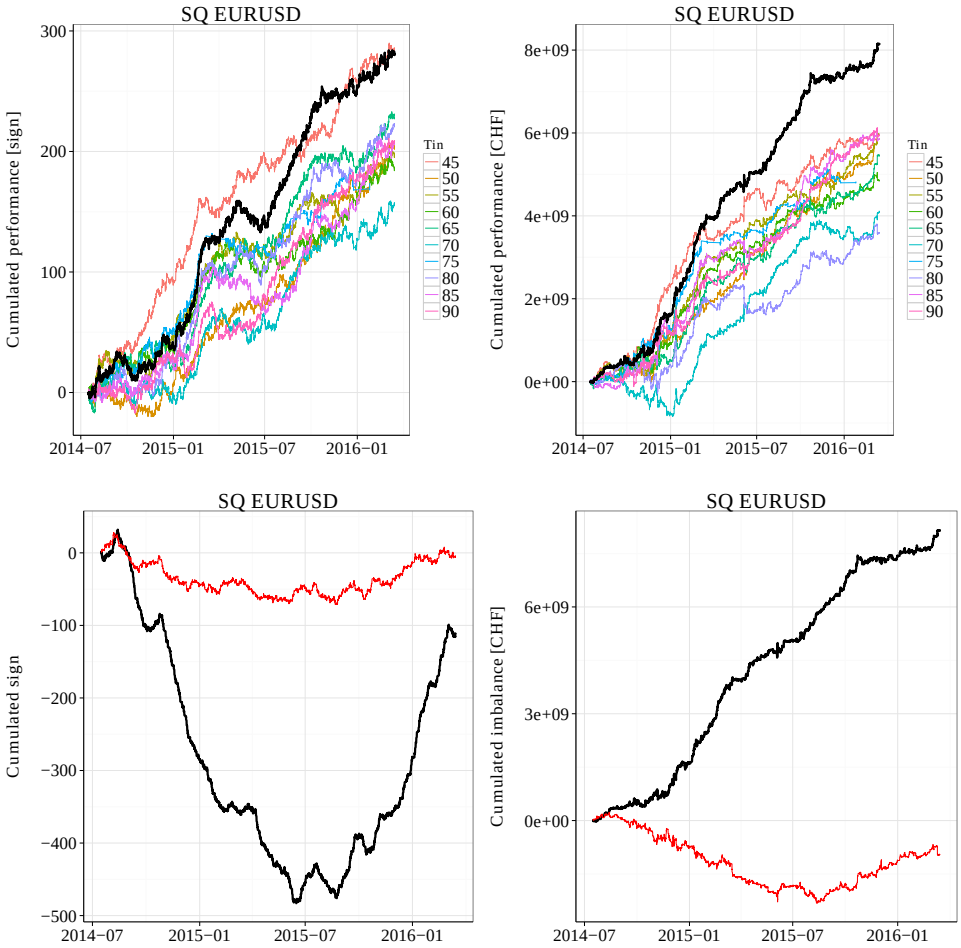

Figure 8: Out-of-sample performance: cumulated product of the predicted order flow sign and actual sign (upper left), cumulated product of the predicted order flow sign and actual order flow (upper right), cumulated product of the predicted order flow sign and actual order flow, and the cumulated actual flow (lower left), cumulated product of the predicted order flow direction and actual order flow (black line) and cumulated actual order flow (red line); `EURUSD`, Swissquote. The thick black lines denote a majority vote between all calibration window lengths.

6.2 Results

We run the procedure on the three most traded pairs of the SQ 2014-6 dataset and on `EURUSD` LB dataset. Figures 8 to 11 report the out-of-sample performance of our method. Although we train RFs on the signs of order flow, we also plot the cumulated performance in currency units. In essence, if the prediction of the order flow signs is successful during the most active periods, it also predicts the actual order flow itself, on average. This the case of SQ clients, but not for LB: the most precise sign predictions are during lunch time, i.e. when the activity reaches a local minimum.

A possible explanation for this is the clear difference between SQ and LB clients: whereas the cumulated net imbalance of SQ clients is mostly mean-reverting, that of LB clients keeps on increasing. This means that SQ clients are mostly speculators, while LB clients use the FX market for other purposes

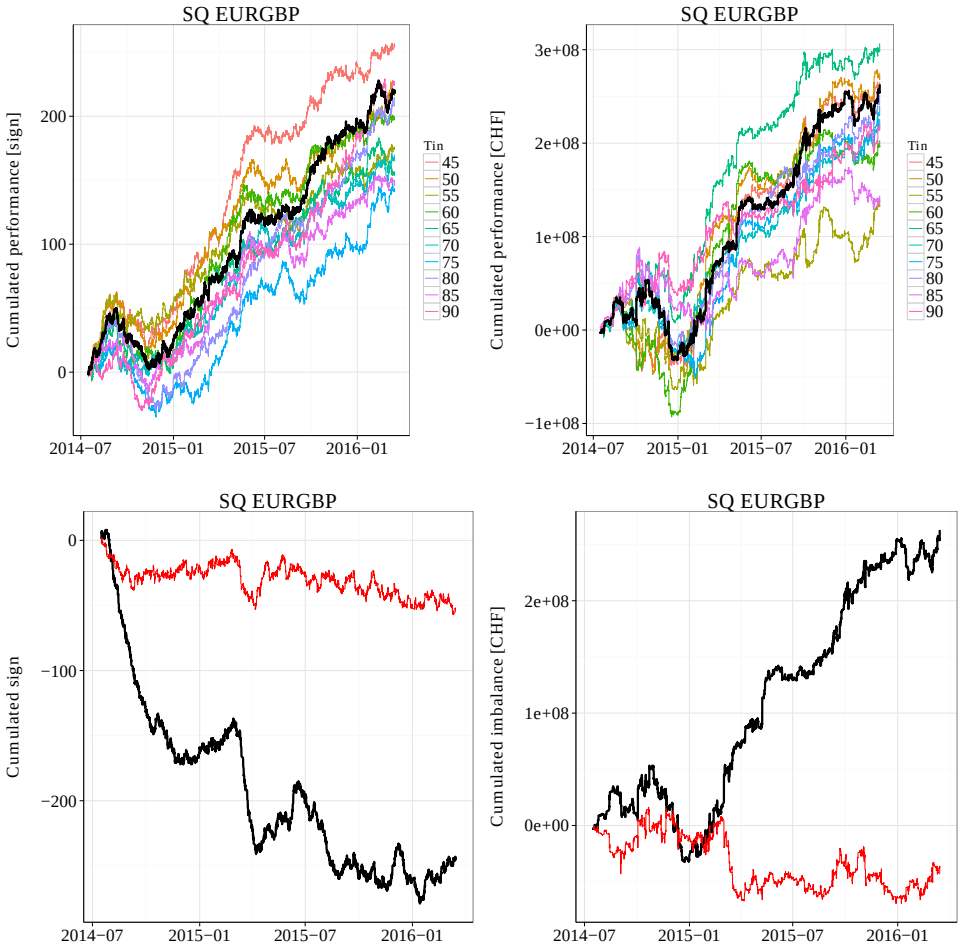

Figure 9: Out-of-sample performance: cumulated product of the predicted order flow sign and actual sign (upper left), cumulated product of the predicted order flow sign and actual order flow (upper right), cumulated product of the predicted order flow sign and actual order flow, and the cumulated actual flow (lower left), cumulated product of the predicted order flow direction and actual order flow (black line) and cumulated actual order flow (red line); `EURGBP`, Swissquote. The thick black lines denote a majority vote between all calibration window lengths.

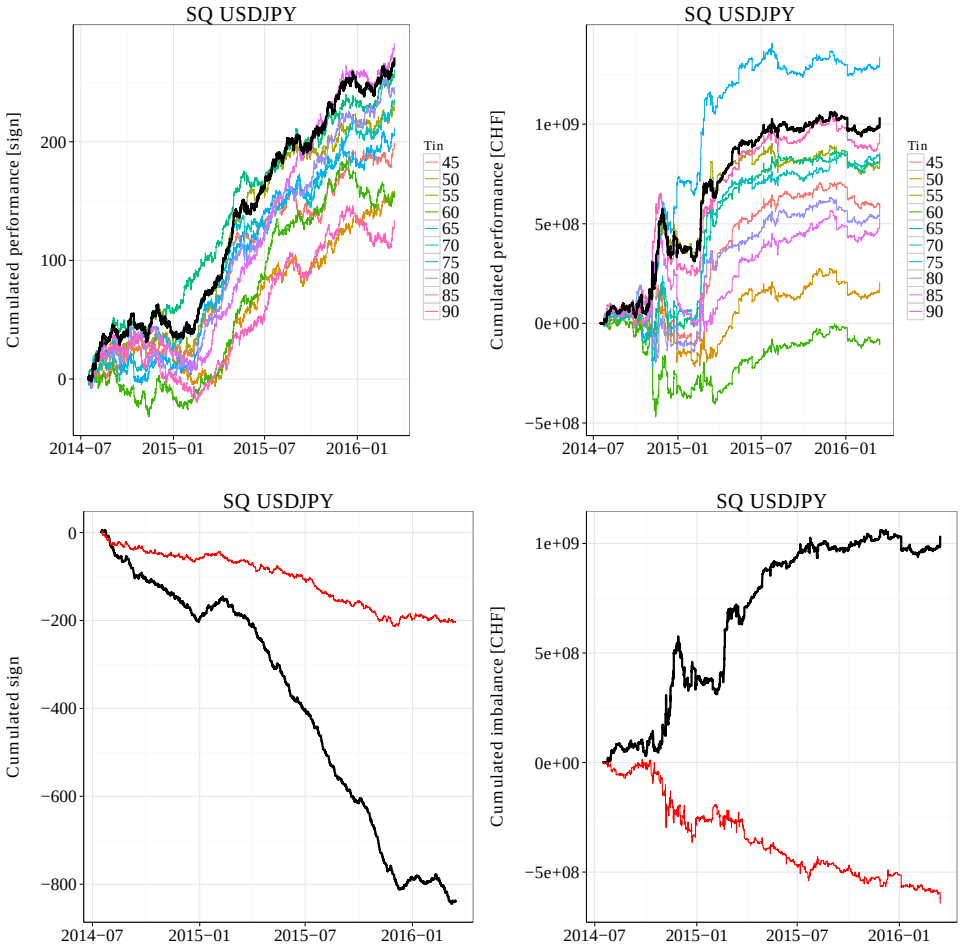

Figure 10: Out-of-sample performance: cumulated product of the predicted order flow sign and actual sign (upper left), cumulated product of the predicted order flow sign and actual order flow (upper right), cumulated product of the predicted order flow sign and actual order flow, and the cumulated actual flow (lower left), cumulated product of the predicted order flow direction and actual order flow (black line) and cumulated actual order flow (red line); `USDJPY`, Swissquote. The thick black lines denote a majority vote between all calibration window lengths.

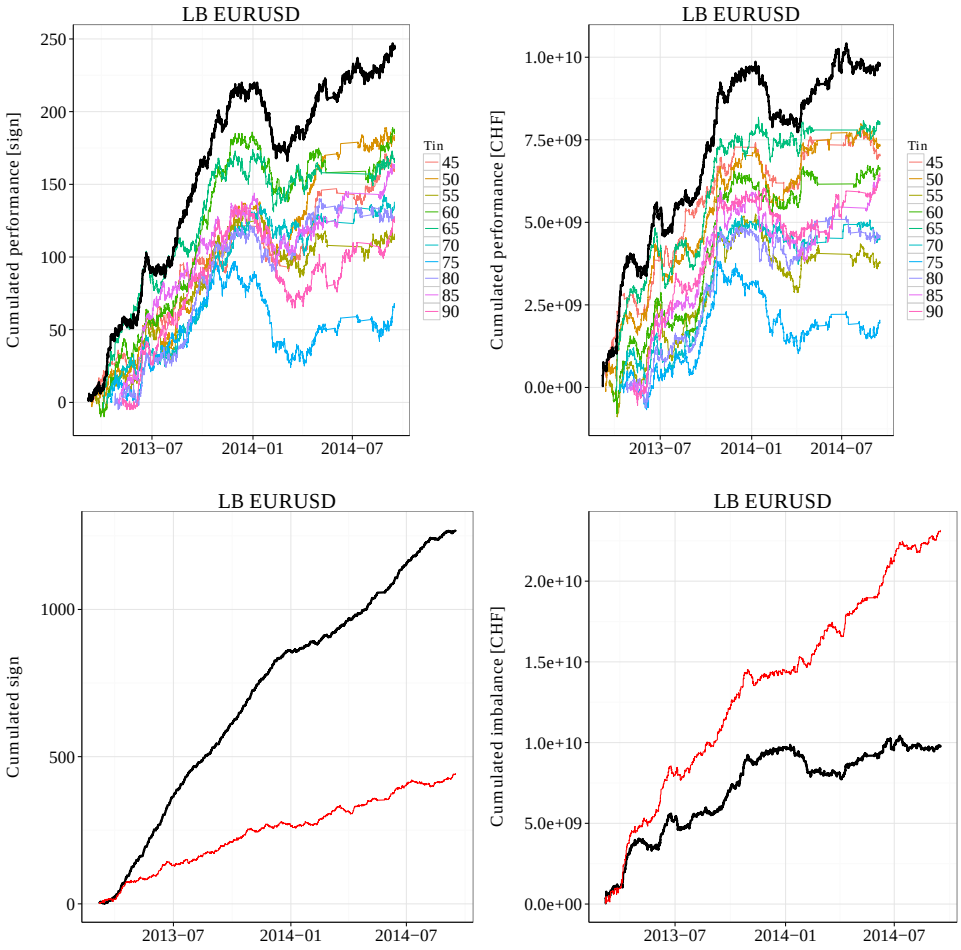

Figure 11: Out-of-sample performance: cumulated product of the predicted order flow sign and actual sign (upper left), cumulated product of the predicted order flow sign and actual order flow (upper right), cumulated product of the predicted order flow sign and actual order flow, and the cumulated actual flow (lower left), cumulated product of the predicted order flow direction and actual order flow (black line) and cumulated actual order flow (red line); `EURUSD`, LB. The thick black lines denote a majority vote between all calibration window lengths.

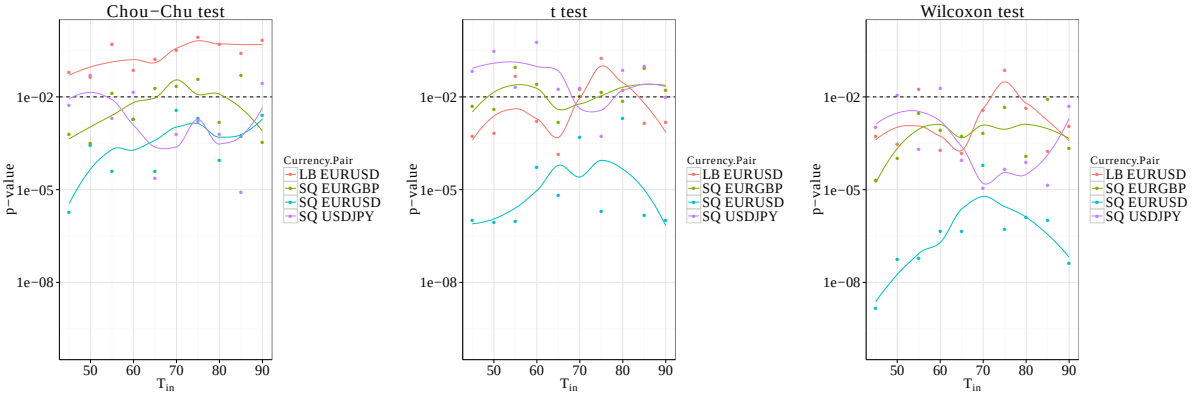

Figure 12: Tests of the predictive power of the binary prediction (left plot) and two tests of the out-of-sample flow prediction performance. Smoothed curves and dashed lines at $y = 0.01$ are for eye-guidance only.

than mere speculation, on average.

Let us now apply basic statistical test to the out-of-sample performance in currency units: for both brokers and all pairs, the out-of-sample performance is clearly significant. However, the real question is the predictive power of our methodology regarding the sign of the next order flow. Chou and Chu approach consists in testing whether A predicts B, where A and B are binomial variables, taking into account auto-correlations, the null hypothesis being that A does not predict B [Chou and Chu, 2010]. When applied to SQ data, this test shows unambiguously that our method yields predictive answers, and that it is not useful in the case of LB data. This may mean that an hourly time scale may not be a wise choice for LB traders.

A different way to look at the results is to analyse the performance conditioned on the hour of the day. In Fig. 13, we report the p-values of out-of-sample performance conditional on the hour of the day. We notice a tendency to perform well in periods of high activity for SQ clients, not for LB clients.

Adding the returns to the feature set did not improve the forecast, probably because the returns effect are already embedded in groups actions, in line with the factor analysis of Lillo et al. [2008]. Remarkably, multiple runs of the procedure revealed that there is no need to update the model every day: an update every 5 days gave approximately the same results, which is consistent with the large persistence, on average, of lead-lag networks.

6.3 Importance of predictors

In order to check that the order flow imbalance depends on the group states we check *a contrario* that the hour of the day is not the most important predictor most of the time. That the non-linear relationship between the predictors and future order imbalance signs sometimes depends on the hour of the day is not surprising, as indeed some groups may be more active at certain times of the day. However, given the existence of lead-lag networks, we do not expect the hour of the day to top the list of variable importance very often.

There are several ways to measure variable importance in Random Forests; we have used the standard Breiman-Cutler measure, which consists (roughly speaking) in shuffling the elements of a given column of the predictors matrix and determining how the in-sample prediction error changes (see Breiman [2001] for more details). We shall focus on the rank of the hour of the day relative to the one of all the other columns. Since we use an unsupervised method to cluster the traders, the number of groups varies as a function of time. As a consequence, we define the rank ratio of column h as the ratio between the rank of the importance of h, denoted by $\mathrm{rank}(h)$, 1 being the most important, and the number of columns of P, denoted by K_{t_1}. Because a rank of 1 would correspond to $1/K_{t_1}$, a time varying quantity, and might therefore make it unnecessarily difficult to compare two rank ratios, we define the adjusted rank ratio of

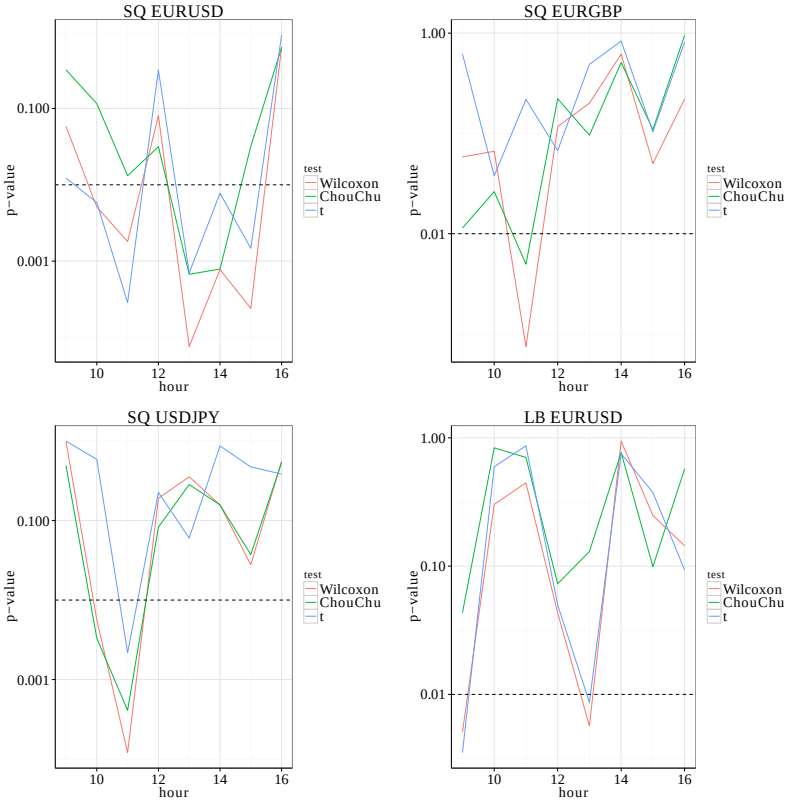

Figure 13: Test of the predictive power of the binary prediction (Chou-Chu) and of the resulting cumulated predicted imbalance (Wilcoxon and t) as a function of the time of the day.

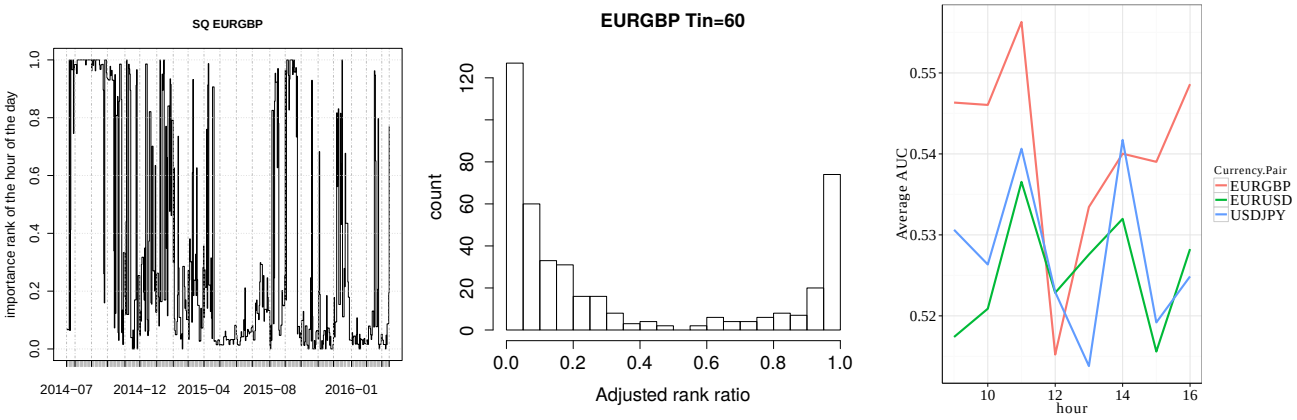

Figure 14: Adjusted rank ratio of importance of the hour of the days, r_h , for EURGBP as a function of time (left plot) and its histogram (middle plot). The right plot reports the dependence on the Area Under Curve (AUC) of r_h, averaged over all T_{in}, as a function the hour of the day. Dataset: SQ2014-6

h as

$$r_h = \frac{\text{rank}(h) - 1}{K_{t_1} - 1}.$$

With this convention, the hour column is the most important predictor if $r_h = 0$ and the least important one if $r_h = 1$. The left plot of Fig 14 plots r_h as a function of time for EURGBP. It turns out that the distribution of the relative importance of h is rather bimodal (see the histogram in the middle plot of the same figure) and persistent. The bimodal nature of r_h is less pronounced for other T_{in} and currency pairs. At all rates, one may wonder if prediction is more successful in periods of low r_h or high r_h, or equivalent, how predictive of success r_h is. As we deal with a classification problem, the tool of choice is Receiver Operating Characteristic (ROC) curves and their associated Area Under Curve (AUC), which, in a nutshell, quantifies how different the distribution of r_h is when the prediction is correct and when it fails. By definition, an AUC of 0.5 corresponds to the absence of predictive power of r_h, while an AUC of 1 implies that r_h fully determines the success of predictions. The right plot of the same figure makes it clear that there is some predictability associated to r_h, and that it is once again larger during the most active hours. Since there is only one value of r_h for each day, and since one makes one prediction per hour, we have computed average AUC conditional on the hour of the day.

Finally, we compute the hourly average AUC of the trader-trader lead-lag persistence β. Figure 15 reports the AUC for the three SQ currency pairs as a function of the number of weeks of the calibration window, restricted to the same out-of-sample period. Once again, the predictive power of such measure is weak.

7 Conclusion and perspectives

Our aim was first to introduce an unsupervised lead-lag network inference method and show the existence of persistent lead-lag networks between groups of investors. This hidden structure may only be inferred from trader-resolved data. Reciprocally, any matching engine may exploit this structure to predict order flow. Although we have only studied the simplest prediction problem and have used standard machine learning methods in the simplest way possible, it turns out that these networks are persistent enough to make investment flow imbalance predictable.

Being able to predict the evolution of one's inventory is useful for improving internal order matching and inventory management, in particular when faced with constraints on maximum exposure. In this

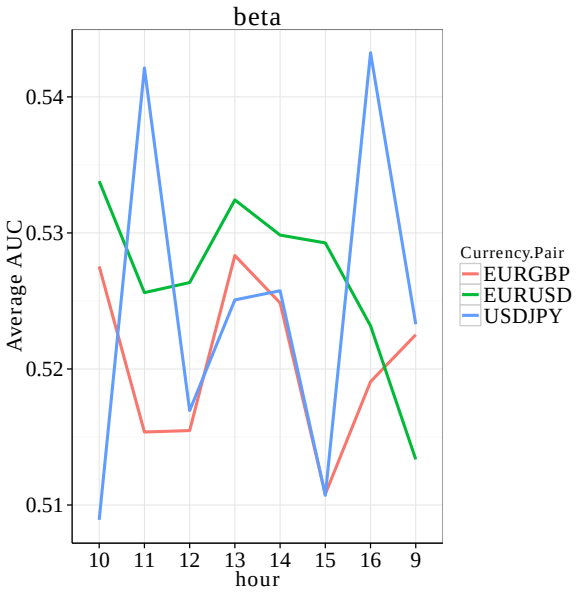

Figure 15: Area Under Curve (AUC) vs the hour of the day for the trader-trader lead-lag persistence measure β; SQ 2014-6 dataset.

respect, being able to predict future price returns from lead-lag networks is needed to build a complete predictive market making system, as the gain of holding an inventory (spared Prime Brokerage fees plus full Bid-Ask spread) must offset the potential directional loss. Future work will address this issue.

So far, we tried to avoid overfitting by averaging the length of the calibration window and only including one step of lag in the group states in the predictors; a better way to exploit the prediction of each calibration window length would be to use on-line learning methods for the aggregation of the prediction of each calibration window length. In addition, there is no doubt that the group states lagged more than once may well be relevant because some traders have typical holding period larger than one hour. We have also avoided method overfitting by using a single machine learning method without trying to vary any of its parameters. Incidentally, we have not exploited the full potential of Random Forests. Indeed, they do not output the sign of the next order flow but an estimate of the probability that it will be positive, negative or zero. Thus, one may abstain to make any prediction when the output probabilities are not significantly biased towards one choice. Finally, variations of this method, such as oblique Random Forests [Menze et al., 2011], or boosted trees [Friedman et al., 2000] may yield better performance.

On a more philosophical note, our work is a first step towards the understanding of what triggers the activity of an investor, one of the current mysteries in Finance. We cannot explain yet why a group of trader acts at time t. However, their activity depends on the past activity of some other groups or themselves. This is a recursive (thus indirect) answer to a question that deserves further investigation.

References

Marco Avellaneda and Sasha Stoikov. High-frequency trading in a limit order book. *Quantitative Finance*, 8(3):217–224, 2008.

B.M. Barber, Y.T. Lee, Y.J. Liu, and T. Odean. Just how much do individual investors lose by trading? *Review of Financial Studies*, 22(2):609–632, 2009.

Yoav Benjamini and Yosef Hochberg. Controlling the False Discovery Rate: A Practical and Powerful Approach to Multiple Testing. *Journal of the Royal Statistical Society. Series B (Methodological)*, 57 (1):289–300, January 1995. ISSN 00359246. doi: 10.2307/2346101. URL `http://www.jstor.org/stable/2346101`.

Jean-Philippe Bouchaud, J. Doyne Farmer, and Fabrizio Lillo. How markets slowly digest changes in supply and demand. In T. Hens and K.R. Schenk-Hoppè, editors, *Handbook of Financial Markets: Dynamics and Evolution*, pages 57–160. Elsevier, 2009.

Jacob Boudoukh, Matthew P Richardson, and RE Whitelaw. A tale of three schools: Insights on autocorrelations of short-horizon stock returns. *Review of financial studies*, 7(3):539–573, 1994.

Leo Breiman. Random Forests. *Machine Learning*, 45(1):5–32, 2001. ISSN 0885-6125. doi: 10.1023/A:1010933404324. URL `http://dx.doi.org/10.1023/A:1010933404324`.

Cheng Chou and Chia-Shang J Chu. Testing independence of two autocorrelated binary time series. *Statistics & probability letters*, 80(1):69–75, 2010.

Aaron Clauset, Cosma Rohilla Shalizi, and Mark EJ Newman. Power-law distributions in empirical data. *SIAM review*, 51(4):661–703, 2009.

Chester Curme, Michele Tumminello, Rosario N Mantegna, H Eugene Stanley, and Dror Y Kenett. Emergence of statistically validated financial intraday lead-lag relationships. *Quantitative Finance*, (ahead-of-print):1–12, 2015.

Manuel Fernández-Delgado, Eva Cernadas, Senén Barro, and Dinani Amorim. Do we Need Hundreds of Classifiers to Solve Real World Classification Problems? *Journal of Machine Learning Research*, 15:3133–3181, 2014. URL `http://jmlr.org/papers/v15/delgado14a.html`.

Chris Fraley, Adrian E. Raftery, T. Brendan Murphy, and Luca Scrucca. mclust version 4 for R: Normal mixture modeling for model-based clustering, classification, and density estimation, 2012.

Jerome Friedman, Trevor Hastie, Robert Tibshirani, et al. Additive logistic regression: a statistical view of boosting (with discussion and a rejoinder by the authors). *The annals of statistics*, 28(2):337–407, 2000.

Florent Gallien, Serge Kassibrakis, Semyon Malamud, and Filippo Passerini. Managing inventory with proportional transaction costs. *Available at SSRN 2788593*, 2016.

Colin S. Gillespie. Fitting heavy tailed distributions: The poweRlaw package. *Journal of Statistical Software*, 64(2):1–16, 2015. URL `http://www.jstatsoft.org/v64/i02/`.

Mark Grinblatt and Matti Keloharju. The investment behavior and performance of various investor types: a study of Finland's unique data set. *Journal of Financial Economics*, 55(1):43–67, 2000.

Mark Grinblatt and Matti Keloharju. Sensation Seeking, Overconfidence, and Trading Activity. *The Journal of Finance*, 64(2):549–578, April 2009. ISSN 1540-6261. doi: 10.1111/j.1540-6261.2009.01443.x. URL `http://dx.doi.org/10.1111/j.1540-6261.2009.01443.x`.

Larry Harris. *Trading and exchanges: Market microstructure for practitioners*. Oxford University Press, 2002.

Nicolas Huth and Frédéric Abergel. High frequency lead/lag relationships–empirical facts. *Journal of Empirical Finance*, 26:41–58, 2014.

H. Ishwaran and U.B. Kogalur. *Random Forests for Survival, Regression and Classification (RF-SRC)*, 2016. URL `https://cran.r-project.org/package=randomForestSRC`. R package version 2.4.1.

A. Jackson. The aggregate behaviour of individual investors. 2004.

Narasimhan Jegadeesh and Sheridan Titman. Overreaction, delayed reaction, and contrarian profits. *Review of Financial Studies*, 8(4):973–993, 1995.

R. Kaniel, G. Saar, and S. Titman. Individual investor trading and stock returns. *The Journal of Finance*, 63(1):273–310, 2008.

Eric K Kelley and Paul C Tetlock. How wise are crowds? insights from retail orders and stock returns. *The Journal of Finance*, 68(3):1229–1265, 2013.

L Kullmann, Janos Kertész, and K Kaski. Time-dependent cross-correlations between different stock returns: A directed network of influence. *Physical Review E*, 66(2):026125, 2002.

Mehdi Lallouache and Frédéric Abergel. Tick size reduction and price clustering in a FX order book. *Physica A: Statistical Mechanics and its Applications*, 416:488–498, 2014.

Andrea Lancichinetti and Santo Fortunato. Community detection algorithms: A comparative analysis. *Phys. Rev. E*, 80(5):56117, November 2009. doi: 10.1103/PhysRevE.80.056117. URL `http://link.aps.org/doi/10.1103/PhysRevE.80.056117`.

F. Lillo and J. D. Farmer. The long memory of efficient markets. *Non-lin. Dyn. and Econometric*, 8, 2004.

Fabrizio Lillo, Esteban Moro, Gabriella Vaglica, and Rosario N Mantegna. Specialization and herding behavior of trading firms in a financial market. *New Journal of Physics*, 10(4):43019, 2008. ISSN 1367-2630. URL `http://stacks.iop.org/1367-2630/10/i=4/a=043019`.

BjoernH. Menze, B.Michael Kelm, DanielN. Splitthoff, Ullrich Koethe, and FredA. Hamprecht. On Oblique Random Forests. In Dimitrios Gunopulos, Thomas Hofmann, Donato Malerba, and Michalis Vazirgiannis, editors, *Machine Learning and Knowledge Discovery in Databases SE - 29*, volume 6912 of *Lecture Notes in Computer Science*, pages 453–469. Springer Berlin Heidelberg, 2011. ISBN 978-3-642-23782-9. doi: 10.1007/978-3-642-23783-6_29. URL `http://dx.doi.org/10.1007/978-3-642-23783-6_29`.

William M Rand. Objective criteria for the evaluation of clustering methods. *Journal of the American Statistical association*, 66(336):846–850, 1971.

Martin Rosvall and Carl T Bergstrom. Maps of random walks on complex networks reveal community structure. *Proceedings of the National Academy of Sciences of the United States of America*, 105(4): 1118–23, January 2008. ISSN 1091-6490. doi: 10.1073/pnas.0706851105. URL `http://www.pnas.org/cgi/content/long/105/4/1118`.

Bence Tóth and János Kertész. Increasing market efficiency: Evolution of cross-correlations of stock returns. *Physica A: Statistical Mechanics and its Applications*, 360(2):505–515, 2006.

Michele Tumminello, Salvatore Miccichè, Fabrizio Lillo, Jyrki Piilo, and Rosario N Mantegna. Statistically Validated Networks in Bipartite Complex Systems. *PLoS ONE*, 6(3):e17994, March 2011. URL `http://dx.doi.org/10.1371/journal.pone.0017994`.

Michele Tumminello, Fabrizio Lillo, Jyrki Piilo, and Rosario N. Mantegna. Identification of clusters of investors from their real trading activity in a financial market. *New Journal of Physics*, 14, 2012. URL `http://iopscience.iop.org/1367-2630/14/1/013041/metrics#.VCl4qVM0YwI.mendeley`.

Wei-Xing Zhou, Guo-Hua Mu, and János Kertesz. Random matrix approach to the dynamics of stock inventory variations. *New Journal of Physics*, 14(9):93025, 2012. ISSN 1367-2630. URL `http://stacks.iop.org/1367-2630/14/i=9/a=093025`.

Ilija Zovko and J. Doyne Farmer. Correlations and clustering in the trading of members of the London Stock Exchange. In *AIP Conference Proceedings*, volume 965, pages 287–299. AIP, 2007. doi: 10.1063/1.2828747. URL `http://scitation.aip.org/content/aip/proceeding/aipcp/10.1063/1.2828747`.

A Prediction with logistic regression

For the sake of meaningful comparisons, we gave to logistic regression the same inputs as to random forests (but split the hour of the day into separate factors), used the same calibration window lengths, and fitted a logistic model every day. The prediction of the model is then rounded to either -1 or +1. The performance summary statistics corresponding to the majority vote between all the calibration window lengths both for logistic regression and random forests fare are reported in Table 4. It is quite clear that logistic regression is out-performed by random forests.

EURCHF	RF	logistic
Chou Chu	3.5e-06	4.8e-05
t	5.0e-12	2.4e-05
Wilcoxon	3.9e-13	1.3e-05

EURGBP	RF	logistic
Chou Chu	8.2e-05	3.6e-04
t	4.7e-03	1.8e-04
Wilcoxon	5.0e-05	4.2e-05

USDJPY	RF	logistic
Chou Chu	4.8e-05	7.9e-01
t	4.7e-03	3.9e-01
Wilcoxon	4.0e-06	1.7e-03

Table 4: P-values of various tests for positive performance for logistic regression and random forests (RF) on SQ2014-6 dataset.